Current Medical Imaging Reviews, 2018, *14*, 416-421

RESEARCH ARTICLE

Dynamic Contrast-enhanced Magnetic Resonance Imaging for Differentiating Between Primary Tumor, Metastatic Node and Normal Tissue in Head and Neck Cancer

Liangliang Chen[1,#], Yufeng Ye[2,3,#], Hanwei Chen[2,3,#], Shihui Chen[1], Jinzhao Jiang[4], Guo Dan[1,*] and Bingsheng Huang[1,*]

[1]*National-Regional Key Technology Engineering Laboratory for Medical Ultrasound, Guangdong Key Laboratory for Biomedical Measurements and Ultrasound Imaging, School of Biomedical Engineering, Health Science Center, Shenzhen University, Shenzhen, China;* [2]*Department of Radiology, Guangzhou Panyu Central Hospital, Guangzhou, China;* [3]*Medical Imaging Institute of Panyu, Guangzhou, China;* [4]*Department of Radiology, The University of Hong Kong Shenzhen Hospital, Shenzhen, China*

ARTICLE HISTORY

Received: July 22, 2017
Revised: November 23, 2017
Accepted: December 04, 2017

DOI:
10.2174/1573405614666171205105236

Abstract: ***Objective*:** To study the difference of the Dynamic Contrast-Enhanced Magnetic Resonance Imaging (DCE-MRI) parameters among the primary tumor, metastatic node and peripheral normal tissue of head and neck cancer.

***Materials and Methods*:** Consecutive newly-diagnosed head and neck cancer patients with nodal metastasis between December 2010 and July 2013 were recruited, and 25 patients (8 females; 24~63 , mean 43±11 years old) were enrolled. DCE-MRI was performed in the primary tumor region including the regional lymph nodes on a 3.0-T MRI system. Three quantitative parameters: K^{trans} (volume transfer constant), v_e (volume fraction of extravascular extracellular space) and k_{ep} (the rate constant of contrast transfer) were calculated for the largest node. A repeated-measure ANOVA with a Greenhouse-Geisser correction and post hoc tests using the Bonferroni correction were used to evaluate the differences in K^{trans}, v_e and k_{ep} among primary tumors, metastatic nodes and normal tissue.

***Results*:** The values of both K^{trans} and v_e of normal tissue differed significantly from those of nodes (both $P < 0.001$) and primary tumors (both $P < 0.001$) respectively, while no significant differences of K^{trans} and v_e were observed between nodes and primary tumors ($P = 0.075$ and 0.365 respectively). The k_{ep} values of primary tumors were significantly different from those of nodes ($P = 0.001$) and normal tissue ($P = 0.002$), while no significant differences between nodes and normal tissue ($P > 0.999$).

***Conclusion*:** The DCE-MRI parameters were different in the tumors, metastatic nodes and normal tissue in head and neck cancer. These findings may be useful in the characterization of head and neck cancer.

Keywords: Head and neck cancer, dynamic contrast-enhanced magnetic resonance imaging, primary tumor, nodal metastasis, normal tissue, quantitative analysis.

1. INTRODUCTION

Head and neck cancer, especially nasopharyngeal carcinoma, is an aggressive cancer type commonly found in Southern China. Regardless of the status of the primary lesion, nodal metastasis is a significant prognostic factor for survival [1]. Hence the accurate detection and the characterization of primary tumor and metastatic nodes are of paramount importance in patient management. The gold standard for nodal metastasis has been pathologic verification of needle biopsies and/or long-lasting clinical or radiographic follow-up of suspected nodes [2]. However, needle biopsy is unable to provide the information of the whole node, while follow-up requires a long period, and more importantly, would delay the possible treatment before confirmation of metastasis. Thus, radiographic imaging is able to provide useful information as it can diagnose metastatic nodes and differentiate the primary tumor and metastatic node from normal tissues.

As a kind of Magnetic Resonance Imaging (MRI), Dynamic Contrast-Enhanced MRI (DCE-MRI) may play a key role as a useful biomarker in the studies of cancer. The three

*Address correspondence to these authors at the National-Regional Key Technology Engineering Laboratory for Medical Ultrasound, Guangdong Key Laboratory for Biomedical Measurements and Ultrasound Imaging, School of Biomedical Engineering, Room A2-508, Health Science Center, Shenzhen University Xili Campus, Shenzhen, China; E-mails: huangb@szu.edu.cn; danguo@ szu.edu.cn

[#]Equal contribution, co-first authors.

1875-6603/18 $58.00+.00

quantitative parameters K^{trans}, v_e and k_{ep} derived by DCE-MRI are frequently used. K^{trans} (in minute^{-1}) is the volume transfer constant of contrast agent from blood plasma to Extravascular Extracellular Space (EES) reflecting both blood plasma flow and permeability; v_e is the volume of EES per unit volume of tissue and k_{ep} (in minute^{-1}) is the flux rate constant of contrast agent from EES to plasma and equal to K^{trans} / v_e [3]. Studies have found DCE-MRI to be useful in differentiating diseased nodes from normal nodes in Head and Neck Squamous Cell Cancer (HNSCC), breast cancer, and cervical cancer [4-6]. In breast cancer, it was found that the 100% increase of DCE-MRI signal intensity in nodes has an accuracy of 83% in differentiating axillary Lymph Node (LN) metastases [7]. In such studies, in the malignant nodes the microvascular permeability and the extravascular extracellular space could be increased. However, no studies have been performed about the differentiation between tumor, metastatic node and normal tissue in head and neck cancer.

It has been shown that DCE-MRI by semi-quantitative and quantitative methods is useful in characterizing the neovasculature and permeability of Nasopharyngeal Carcinoma (NPC) [8]. In this study, the perfusion parameters were found to be higher in high stage tumors. However, it is still unclear whether and how DCE-MRI can differentiate between primary tumor, metastatic nodes and normal tissue. Studies have been performed to investigate the usefulness of several imaging techniques, Including Intravoxel Incoherent Motion Imaging (IVIM), Diffusion Weighted Imaging (DWI), and Computed Tomography (CT) perfusion for nodal characterization in head and neck cancer [9-11]. However in these studies only the difference between primary tumor and metastatic nodes, or between normal and metastatic nodes, were studied. In the present project, we aimed to study the difference of DCE-MRI parameters between primary tumor, metastatic nodes and normal tissue. We hypothesized that the DCE-MRI parameters in nodes and in primary tumor are higher than those in normal tissue.

2. MATERIALS AND METHODS

2.1. Patients

This study was approved by the local Institutional Review Board. All consecutive newly-diagnosed head and neck cancer patients between December 2010 and July 2013 were included. Twenty-five patients (8 females; 24~63, mean 43±11 years old) were enrolled. Written informed consent was obtained for each patient before the MRI scan. TNM staging was performed according to the American Joint Committee on Cancer (AJCC) staging system [12].

2.2. MRI Acquisition

DCE-MRI was performed in the primary tumor region including the loco-regional LNs on a 3.0-T system (Magnetom Trio, Siemens) by using a fast 3D spoiled gradient-echo sequence. Imaging parameters were: reconstructed FOV = 260 × 260 mm^2, 20 axial sections, section thickness = 3 mm, FA = 20°, TR/TE = 5.0/4.2 ms. This data-acquisition scheme resulted in a temporal resolution of 4.5 seconds in 4.5 minutes (60 time points) with full spatial resolution of 256 × 256. A single dose of gadodiamide (Gd-DTPA) (Omniscan; Nycomed, Oslo, Norway) at a concentration of 0.1 mmol/kg body weight was injected at the rate of 1 mL/s into the antecubital vein, followed by a saline flush with a power injector (Spectris; Medrad, Indianola, Pennsylvania) at 8th scan. Baseline images were acquired with FA of 5°, 10° and 15° for quantitative analysis of DCE-MRI images. Contrast-Enhanced MRI and T2W-MRI were performed as for routine practice, and used for the following analysis in our study. After DCE-MRI scan, contrast-enhanced MRI were performed with: acquired matrix = (305~335) × (304~332), reconstructed FOV = 220~240 mm, section thickness = 2~3 mm, FA = 10°, TR/TE = 4.7~5.0/2.4~2.5 ms. T2W-MRI were performed with a Inversion Recovery sequence and these parameters: acquired matrix = (210~230) × (260~280), reconstructed FOV = 220~240 mm, section thickness = 3 mm, FA = 90°, TR/TE = 4900~5900/60 ms, number of average = 2.

2.3. ROI Drawing

For each patient, the head and neck cancer tumor boundary was identified in the relevant consecutive slices of the DCE-MRI images and a series of two-dimensional Regions of Interest (ROI) were extracted that included the whole tumor using the software ImageJ (NIH, Bethesda, MD, USA). The largest metastatic node within the scanned region in each patient identified by a neuroradiologist (J Jiang) on conventional anatomical MR images (T1-weighted, T2-weighted, and post-contrast T2-weighted) was taken to be representative of all the metastatic nodes [13-15]. The node boundary was then identified in the relevant consecutive slices of the DCE-MRI images and a series of two-dimensional ROI were contoured in ImageJ. The ROIs on the normal longus capitis muscle were delineated adjacent to both sides of the NPC lesions, and were used for comparison with the tumor and metastatic nodes. This is because the perfusion characteristics of this muscle are similar to the non-tumoral tissue in this region, however an ROI is hard to be drawn within this small region. The criteria for ROI drawing of normal longus capitis muscle were the hypointensity on T2W images and unobvious enhancement on contrast-enhanced T1W images. For the ROI drawing of normal tissue, the areas with hyperintensity on T2W images and/or obvious enhancement on contrast-enhanced T1W images indicate tumor invasion, and hence were avoided when the ROIs were delineated. The ROIs of a typical case is shown in Fig. (**1**).

2.4. Statistical Analysis

The gold standard for nodal metastases in our cohort was clinical and radiographic follow-up of suspected nodes lasting for at least 2 years [16]. The parametric maps of K^{trans}, v_e and k_{ep} were calculated from the acquired DCE-MRI images according to Huang *et al*. [8]. The whole procedure of calculating parametric maps of K^{trans}, v_e and k_{ep} were performed using the software dcemri S4 (http://cran.r-project.org/web/packages/dcemriS4/) developed by Whitcher *et al*. [17], according to the standard Tofts-Kety model [3]. We directly calculated the arterial input function from the DCE-MRI images of the carotid artery, and if in some patients the individual AIF could not be differentiated clearly, the population AIF acquired from other patients was used [8].

The normality of the DCE-MRI parameters distribution in our cohort was checked using the Shapiro–Wilk test. A

repeated-measure ANOVA with a Greenhouse-Geisser correction and post hoc tests using the Bonferroni correction were used to evaluate the difference in K^{trans}, v_e and k_{ep} among primary tumors, metastatic nodes and normal tissue. All statistical analyses were performed using SPSS 20 (SPSS Inc, Chicago, IL, USA), and $P < 0.05$ was considered statistically significant.

3. RESULTS

The cohort characteristics of this study are shown in Table **1**. There were 10 patients with nasopharyngeal carcinoma, 8 with oropharynx cancer, 3 with cancer in the tongue base, and 4 with cancer of the larynx.

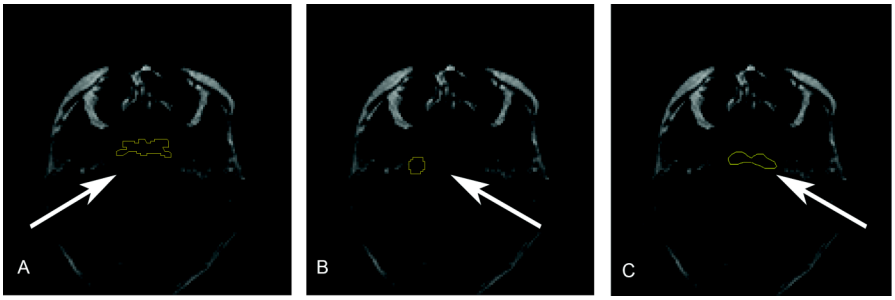

Fig. (1). The ROIs drawn in the MRI images of a typical case for: **A**, the primary tumor; **B**, a metastatic node; **C**, the normal longus capitis muscle.

Table 1. Patient demographic data and tumor characteristics (n=25).

No.	Age	Sex	AJCC Stage	Metastatic Node			Primary Tumor			Normal Tissue		
				K^{trans}	v_e	k_{ep}	K^{trans}	v_e	k_{ep}	K^{trans}	v_e	k_{ep}
1	40	F	4	0.699	0.237	0.103	0.214	0.283	0.762	0.357	0.078	0.229
2	31	M	4	0.175	0.419	0.132	0.207	0.283	0.847	0.100	0.294	0.158
3	46	M	3	0.245	0.348	0.539	0.213	0.341	0.626	0.109	0.158	0.516
4	43	F	4	0.324	0.460	0.369	0.254	0.375	0.473	0.061	0.104	0.645
5	61	M	4	0.445	0.459	0.526	0.240	0.247	1.055	0.247	0.478	0.218
6	58	M	3	0.210	0.222	1.042	0.180	0.248	0.854	0.124	0.159	0.588
7	55	F	3	0.249	0.432	0.623	0.175	0.256	0.786	0.096	0.221	0.510
8	50	M	2	0.257	0.302	0.661	0.164	0.265	0.671	0.143	0.133	0.485
9	36	F	3	0.236	0.365	0.666	0.185	0.273	0.762	0.140	0.157	0.535
10	26	M	3	0.429	0.597	0.527	0.266	0.406	0.629	0.211	0.205	0.464
11	45	F	3	0.459	0.602	0.291	0.280	0.321	0.946	0.256	0.289	0.309
12	45	M	4	0.607	0.623	0.416	0.476	0.492	0.445	0.224	0.495	0.310
13	38	M	3	0.324	0.526	0.518	0.390	0.509	0.699	0.268	0.475	0.215
14	45	F	4	0.293	0.376	0.312	0.300	0.395	0.625	0.025	0.047	0.675
15	28	M	4	0.311	0.328	0.635	0.298	0.415	0.587	0.281	0.406	0.320
16	46	M	3	0.274	0.372	0.594	0.202	0.274	0.731	0.065	0.120	0.495
17	25	M	3	0.338	0.322	0.381	0.251	0.411	0.297	0.053	0.059	0.742
18	40	M	4	0.328	0.380	0.507	0.314	0.368	0.640	0.138	0.229	0.634
19	44	F	3	0.312	0.391	0.299	0.263	0.318	0.650	0.094	0.069	0.481
20	35	M	3	0.256	0.384	0.311	0.283	0.439	0.565	0.117	0.242	0.290
21	60	F	4	0.478	0.419	0.215	0.278	0.351	0.596	0.186	0.107	0.191
22	47	M	4	0.316	0.549	0.384	0.284	0.429	0.500	0.239	0.510	0.234
23	64	M	3	0.234	0.332	0.318	0.308	0.436	0.538	0.258	0.353	0.282
24	52	M	4	0.165	0.344	0.319	0.307	0.356	0.371	0.087	0.137	0.522
25	43	M	3	0.331	0.410	0.427	0.252	0.344	0.620	0.158	0.231	0.418

Age (years), patient age at diagnosis; M, male; F, female; AJCC stage, tumor stage evaluated according to AJCC staging system.
AJCC, American Joint Committee on Cancer.

The mean K^{trans} values of primary tumors, nodes and normal tissue were 0.251±0.066 min^{-1}, 0.332±0.149 min^{-1}, 0.159±0.087 min^{-1} respectively; the mean v_e values were 0.344±0.081, 0.408±0.124 and 0.229±0.146 respectively; and the mean k_{ep} values were 0.621±0.195 min^{-1}, 0.429±0.206 min^{-1} and 0.420±0.170 min^{-1} respectively. As shown in Fig. (**2**), K^{trans}, v_e and k_{ep} differed among different tissue types. Both K^{trans} and v_e of normal tissue differed significantly from those of metastatic nodes (both $P < 0.001$) and primary tumors (both $P < 0.001$), while no significant differences of K^{trans} and v_e were observed between metastatic nodes and primary tumors ($P = 0.075$ and 0.365 respectively). The k_{ep} values of primary tumors were significantly different from those of node ($P = 0.001$) and normal tissue ($P = 0.002$), however no significant differences between those of nodes and normal tissue ($P > 0.999$).

4. DISCUSSION

Studies have been performed to investigate the role of DCE-MRI in differentiating the primary tumors and nodal status from benign tissue in some cancer types. The slopes derived from Time-Intensity Curves (TICs) from DCE-MRI were found to be significantly greater compared to the benign lesions in the tumors of the tongue [18]. Wendl found that in DCE-MRI the mean Time To Peak (TTP) was 27 s (range 18-36 s, SD 9 s) for benign and 21 s (range 18-27 s, SD 5 s) for malignant LNs, and the relative signal change with respect to the reference tissue was significantly higher for LNs with than for those without metastases [19]. In thyroid tumors, the thyroid carcinoma showed significantly lower slope of the rising part of TIC and higher TTP than the benign lesions [20]. In minor salivary gland tumors in the oral cavity, it was also found that the TTP was significantly different between the benign and malignant tumors [21]. By converting the TIC patterns into a color-coded map, it was found that DCE-MRI of head and neck tumors was able to distinguish all 21 primary tumors and 15 metastatic nodes from normal structures [22]. All these studies have justified the role of DCE-MRI in the differentiating diagnosis of cancer. However, none of these publications was related to the role of DCE-MRI quantitative parameters in differentiating the tumor and nodal metastasis from normal tissues of head and neck cancer. We in this study by applying the quantitative analysis of contract concentration curves, calculated the perfusion parameters, and analyzed the role of differentiating among the three tissue types.

In the present study, the K^{trans} of the tumors and metastatic nodes was significantly higher than that of normal issue, which is consistent with the results of Chang *et al*. [23] and Li *et al*. [24]. Chang *et al*. reported that K^{trans} in esophageal adenocarcinoma was higher than in benign tissue, while Li *et al*. found that K^{trans} calculated by a shutter-speed model provided the most useful biomarkers for malignant/benign prostate tissue discrimination. Lowry *et al*. [25] also have a similar finding that K^{trans} in prostate tumor was increased compared to the peripheral normal tissue. The explanation is, K^{trans} is a rate constant measuring the contrast transfer between the intravascular space and the interstitial space within the tissue of interest. With cancer-related angiogenesis, the contrast within tumor blood vessels may exhibit increased permeability thereby allowing a more rapid transfer, when compared to benign tissue, and hence a higher K^{trans} value in tumor or metastatic nodes.

The v_e of tumor was significantly higher compared to the normal issue, consistent with the results by Lowry *et al*. [25], who found that v_e in prostate tumor was increased compared to the peripheral normal tissue. v_e is the measurement of volume of EES per unit volume of tissue, and reflects the available space for contrast permeability. Parallel to the increase of K^{trans} value in tumor and metastatic nodes, our results indicated that the increase of v_e reflects the increase of contrast permeability in tumor and metastatic nodes compared to healthy tissue in head and neck cancer.

Similar to Li *et al*. [24], Lowry *et al*. [25] and Kiessling *et al*. [26], we found that the k_{ep} of tumor was significantly higher compared to the normal tissue. According to Li *et al*., k_{ep} was also useful in discriminating malignant prostate tumor from benign prostate tissue. Lowry *et al*. found that the fast exchange limit model revealed increased mean k_{ep} in tumor compared to the peripheral normal tissue. Kiessling *et al*. reported that k_{ep} of prostate tumors were significantly higher than peripheral non-affected prostate tissue. k_{ep} is a complex parameter depending on the underlying physiology such as blood flow and permeability surface area product. Compared to benign tissues, the microvessel density and

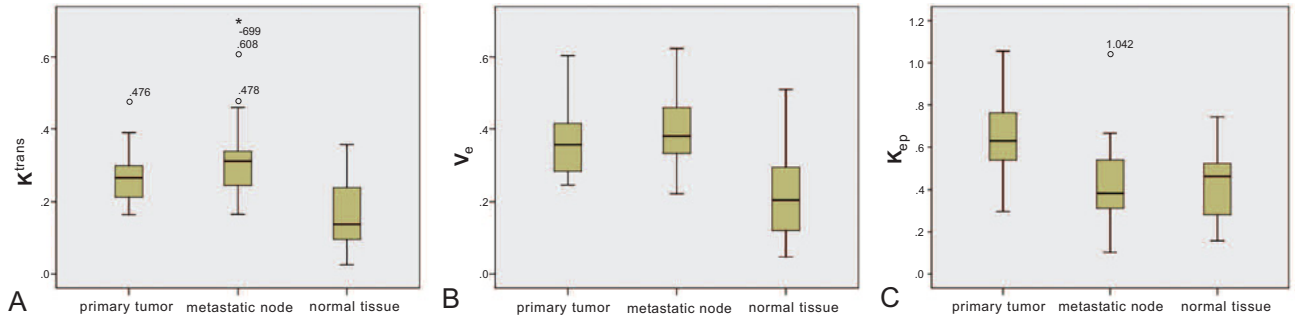

Fig. (2). A: Box plot shows significantly lower K^{trans} (in min^{-1}) of normal tissue compared to primary tumors and metastatic nodes (both $P < 0.001$), and no significant differences of K^{trans} between nodes and primary tumors ($P = 0.075$) by post hoc tests using Bonferroni correction. **B**: Box plot shows significantly lower v_e of normal tissue compared to primary tumors and metastatic nodes (both $P < 0.001$), and no significant differences of v_e between nodes and primary tumors ($P = 0.365$) by post hoc tests using the Bonferroni correction. **C**: Box plot shows significantly higher k_{ep} (in min^{-1}) of primary tumors compared to metastatic nodes and normal tissue ($P = 0.001$ and 0.002 respectively), and no significant differences of k_{ep} between nodes and normal tissue ($P > 0.999$) by post hoc tests using the Bonferroni correction.

vessel permeability of tumors are relatively high, and hence may result in a higher k_{ep}. The k_{ep} showed no significant differences between the tumor and the nodes, which may be because it is calculated as K^{trans} / v_e, and the increase of K^{trans} may be compensated by the increase of v_e.

To summarize, all the results about K^{trans}, v_e and k_{ep} may show that, for our head and neck cancer cohort, the perfusion and vascular permeability in the metastatic LNs were increased, together with the primary tumors. These findings may further indicate that to characterize the head and neck cancer the studies focused on the nodes (but not only on primary tumors) should be performed. Our results in the present study may have some indications for the management of head and neck cancer patients. It has been reported that, the LN status is a key prognostic factor for head and neck cancer [1, 27-29]. In this case, the studies to investigate the perfusion and permeability characteristics in metastatic LNs may play a more important role in the management of head and neck cancer patients.

Our study may have some limitations. Firstly, for each patient, we only selected the largest node in the DCE-MRI scan region. These selection criteria may not be sufficient enough to reflect the status of all nodes. Since some other metastatic nodes were too small to be analyzed, we followed the methodology in the literature and analyzed the largest one only. Secondly, error may be caused by the ROI selection of normal tissue which can be a bit ambiguous among different researchers. However, according to the histological characteristics of head and neck cancer, it was believed that the normal longus capitis muscle be the best choice for comparison. Finally, the sample size was small, thus the statistical power may not be high enough. A large sample would provide more reliable results to verify our findings.

CONCLUSION

Significant differences of K^{trans}, v_e and k_{ep} were observed among the primary tumors, metastatic nodes and normal tissue. We hence concluded that these DCE-MRI parameters may help to differentiate the tumors/metastatic nodes from normal tissue in head and neck cancer. Further studies with bigger cohort are required for validating our findings.

ETHICS APPROVAL AND CONSENT TO PARTICIPATE

This study was approved by the Institutional Review Board. TNM staging was performed according to the American Joint Committee on Cancer (AJCC) staging system.

HUMAN AND ANIMAL RIGHTS

No animal were used in this study, Reported experiments on humans were in accordance with the ethical standards of the committee responsible for human experimentation (institutional national), and with the Helsinki Declaration of 1975, as revised in 2008 (http://www.wma.net/en/20activities/10ethics/10helsinki/).

CONSENT FOR PUBLICATION

Written informed consent was obtained for each patient.

CONFLICT OF INTEREST

The authors declare no conflict of interest, financial or otherwise.

ACKNOWLEDGEMENTS

This study was jointly funded by Guangdong Scientific Research Funding in Medicine (No. B2016031), Shenzhen High-caliber Personnel Research Funding (No. 000048), Special Funding Scheme for Supporting the Innovation and Research of Shenzhen High-caliber Overseas Intelligent (No. KQCX20140519103243534), Shenzhen Municipal Scheme for Basic Research (No. JCYJ20160307114900292; No. JCYJ20160608173106220).

REFERENCES

[1] Han L, Lin SJ, Pan JJ, *et al.* Prognostic factors of 305 nasopharyngeal carcinoma patients treated with intensity-modulated radiotherapy. Chin J Cancer 2010; 29(2): 145-50.

[2] Heeren PA, Jager PL, Bongaerts F, *et al.* Detection of distant metastases in esophageal cancer with 18F-FDG PET. J Nucl Med 2004; 45(6): 980-7.

[3] Tofts PS, Brix G, Buckley DL, *et al.* Estimating kinetic parameters from dynamic contrast-enhanced T(1)-weighted MRI of a diffusable tracer: standardized quantities and symbols. J Magn Reson Imag 1999; 10(3): 223-32.

[4] Sumi M and Nakamura T Extranodal spread in the neck: MRI detection on the basis of pixel-based time-signal intensity curve analysis. J Magn Reson Imag 2011; 33(4): 830-8.

[5] Bhooshan N, Giger ML, Jansen SA, *et al.* Cancerous breast lesions on dynamic contrast-enhanced MR images: computerized characterization for image-based prognostic markers. Radiology 2010; 254(3): 680-90.

[6] Fischbein NJ, Noworolski SM, Henry RG, *et al.* Assessment of metastatic cervical adenopathy using dynamic contrast-enhanced MR imaging. AJNR Am J Neuroradiol 2003; 24(3): 301-11.

[7] Kvistad KA, Rydland J, Smethurst HB, *et al.* Axillary lymph node metastases in breast cancer: preoperative detection with dynamic contrast-enhanced MRI. Eur Radiol 2000; 10(9): 1464-71.

[8] Huang B, Wong CS, Whitcher B, *et al.* Dynamic contrast-enhanced magnetic resonance imaging for characterising nasopharyngeal carcinoma: comparison of semiquantitative and quantitative parameters and correlation with tumour stage. Eur Radiol 2013; 23(6): 1495-502.

[9] Ali TFT. Neck lymph nodes: Characterization with diffusion-weighted MRI. Egypt J Radiol Nucl Med 2012; 43(2): 173-81.

[10] Lu Y, Jansen JF, Stambuk HE, *et al.* Comparing primary tumors and metastatic nodes in head and neck cancer using intravoxel incoherent motion imaging: A preliminary experience. J Comput Assis Tomograp 2013; 37(3): 346-52.

[11] Zhong J, Lu Z, Xu L, *et al.* The diagnostic value of cervical lymph node metastasis in head and neck squamous carcinoma by using diffusion-weighted magnetic resonance imaging and computed tomography perfusion. BioMed Res Internat 2014; 2014.

[12] Edge SBB, D.R.; Compton, C.C.; Fritz, A.G.; Greene, F.L.; Trotti, A., Byrd DR, Compton CC, eds. AJCC Cancer Staging Manual, 7 edn. New York: Springer; 2010.

[13] Jansen JF, Schoder H, Lee NY, *et al.* Tumor metabolism and perfusion in head and neck squamous cell carcinoma: Pretreatment multimodality imaging with (1)h magnetic resonance spectroscopy, dynamic contrast-enhanced MRI, and [(18)F]FDG-PET. Int J Radiat Oncol Biol Phys 2011; 82(1): 299-307.

[14] Chawla S, Kim S, Loevner LA, *et al.* Prediction of disease-free survival in patients with squamous cell carcinomas of the head and neck using dynamic contrast-enhanced MR imaging. AJNR Am J Neuroradiol 2011; 32(4): 778-84.

[15] Kim S, Loevner LA, Quon H, *et al.* Prediction of response to chemoradiation therapy in squamous cell carcinomas of the head and neck using dynamic contrast-enhanced MR imaging. AJNR Am J Neuroradiol 2010; 31(2): 262-8.

[16] de Jong IJ, Pruim J, Elsinga PH*, et al.* Preoperative staging of pelvic lymph nodes in prostate cancer by 11C-choline PET. J Nucl Med 2003; 44(3): 331-5.

[17] Whitcher B, Schmid VJ. Quantitative analysis of dynamic contrast-enhanced and diffusion-weighted magnetic resonance imaging for oncology in R. J Statis Software 2011; 44(5): 1-29.

[18] Ai S, Zhu W, Liu Y*, et al.* Combined DCE and DW-MRI in the diagnosis of benign and malignant tumors of the tongue. Front Bioscie 2013; 18: 1098-111.

[19] Wendl CM, Müller S, Meier J*, et al.* High resolution contrast-enhanced ultrasound and 3-tesla dynamic contrast-enhanced magnetic resonance imaging for the preoperative characterization of cervical lymph nodes: First results. Clin Hemorheol Microcirculat 2012; 52(2): 153-66.

[20] Yuan Y, Yue X-H, Tao X-F. The diagnostic value of dynamic contrast-enhanced MRI for thyroid tumors. Eur J Radiol 2012; 81(11): 3313-8.

[21] Matsuzaki H, Yanagi Y, Hara M*, et al.* Minor salivary gland tumors in the oral cavity: Diagnostic value of dynamic contrast-enhanced MRI. Eur J Radiol 2012; 81(10): 2684-91.

[22] Yuan J, Chow S, Yeung D*, et al.* A five-colour colour-coded mapping method for DCE-MRI analysis of head and neck tumours. Clin Radiol 2012; 67(3): 216-23.

[23] Chang EY, Li X, Jerosch-Herold M*, et al.* The evaluation of esophageal adenocarcinoma using dynamic contrast-enhanced magnetic resonance imaging. J Gastrointest Surg 2008; 12(1): 166-75.

[24] Li X, Priest RA, Woodward WJ*, et al.* Feasibility of shutter-speed DCE-MRI for improved prostate cancer detection. Magn Reson Med 2013; 69(1): 171-8.

[25] Lowry M, Zelhof B, Liney GP*, et al.* Analysis of prostate DCE-MRI: comparison of fast exchange limit and fast exchange regimen pharmacokinetic models in the discrimination of malignant from normal tissue. Invest Radiol 2009; 44(9): 577-84.

[26] Kiessling F, Lichy M, Grobholz R*, et al.* Simple models improve the discrimination of prostate cancers from the peripheral gland by T1-weighted dynamic MRI. Eur Radiol 2004; 14(10): 1793-801.

[27] Aribas BK, Cetindag F, Ozdogan Z*, et al.* Nasopharyngeal carcinomas: prognostic factors and treatment features. J Egypt Natl Canc Inst 2008; 20(3): 230-6.

[28] Ma J, Liu L, Tang L*, et al.* Retropharyngeal lymph node metastasis in nasopharyngeal carcinoma: Prognostic value and staging categories. Clin Cancer Res 2007; 13(5): 1445-52.

[29] Tang L, Li L, Mao Y*, et al.* Retropharyngeal lymph node metastasis in nasopharyngeal carcinoma detected by magnetic resonance imaging: Prognostic value and staging categories. Cancer 2008; 113(2): 347-54.